SP 1450 Ice-shelf deflections modelled with a full 3D elastic model

Y.V. Konovalov

National Research Nuclear University "MEPhI", Kashirskoe shosse 31, 115409 Moscow, Russian Federation, e-mail: yu-v-k@yandex.ru.

1. Introduction

Ice-shelf flexure modelling was performed using a full 3D finite-difference elastic model, which takes into account sub-ice-shelf seawater flow. The sub-ice seawater flow was described by the wave equation (Holdsworth and Glynn, 1978), so the ice-shelf flexures result from the hydrostatic pressure perturbations in sub-ice seawater. The modelling of ice-shelf vibrations was successfully performed in (Holdsworth and Glynn, 1978) by employing of the thin-plate approximation. The numerical simulation has shown that the modelling of the ice-shelf vibrations can be performed in the full model, which links well known momentum equations with the wave equation for non-viscous fluid, i.e. for sub-ice seawater. Nevertheless, the numerical simulation reveals that the numerical solution stability requires the application of an additional method in the numerical approximation. The aim of this work is in an attempt to apply an additional approximation in the boundary conditions to improve the numerical stability of the model.

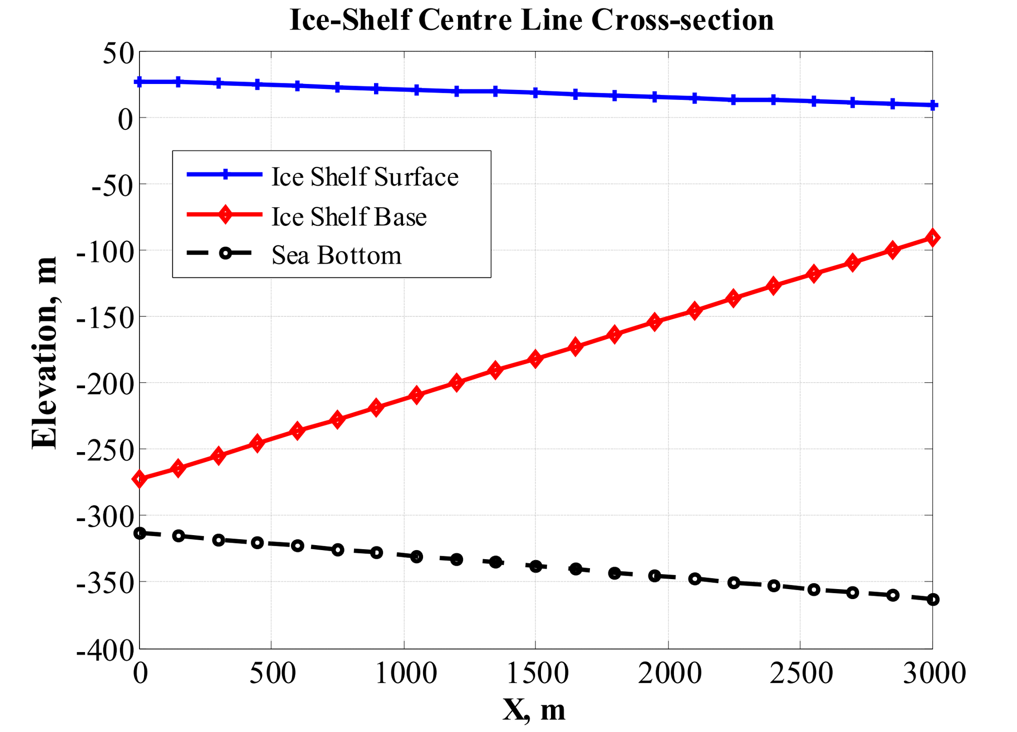

Fig. 1. Ice-shelf center line profile, which has trapezoidal shape and which was applied in the numerical experiments.

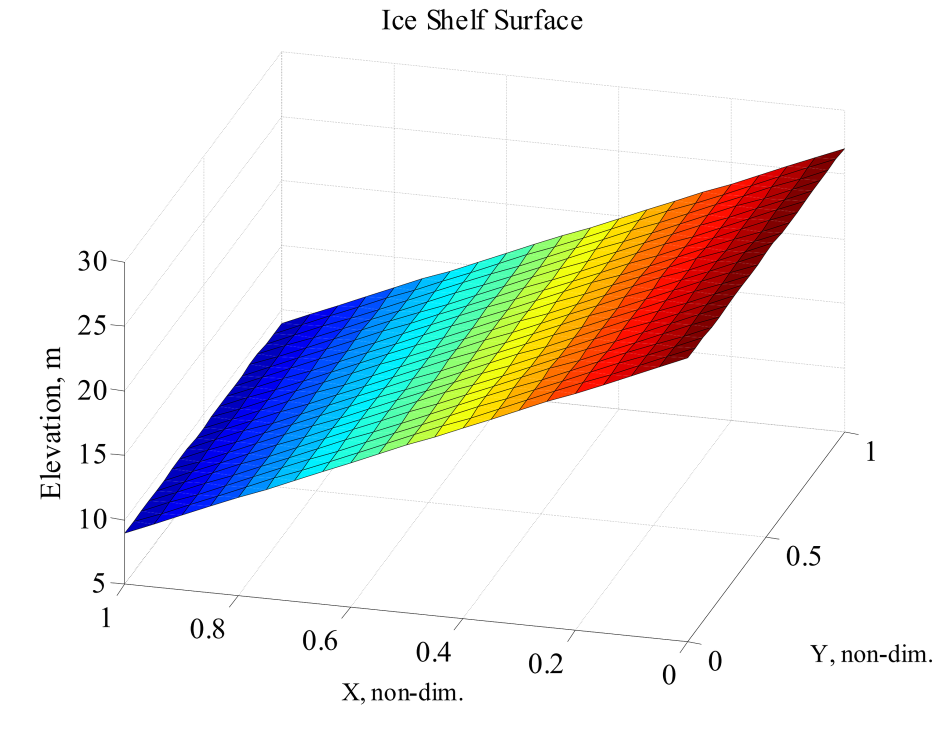

Fig. 1. Ice-shelf geometry (ice-shelf surface) applied in the numerical experiments.

2. Field equations

Basic equations

Momentum equations:

$$\begin{cases} \dfrac{\partial \sigma_{xx}}{\partial x}+\dfrac{\partial \sigma_{xy}}{\partial y}+\dfrac{\partial \sigma_{xz}}{\partial z}=\rho\dfrac{\partial^2 U}{\partial t^2}; \\ \dfrac{\partial \sigma_{yx}}{\partial x}+\dfrac{\partial \sigma_{yy}}{\partial y}+\dfrac{\partial \sigma_{yz}}{\partial z}=\rho\dfrac{\partial^2 V}{\partial t^2}; \\ \dfrac{\partial \sigma_{zx}}{\partial x}+\dfrac{\partial \sigma_{zy}}{\partial y}+\dfrac{\partial \sigma_{zz}}{\partial z}=\rho\, g+\rho\dfrac{\partial^2 W}{\partial t^2}; \\ 0<x<L; y_1(x)<y<y_2(x); h_b(x,y)<z<h_s(x,y) \end{cases}$$

where σ_{ik} is stress tensor, U,V,W are two horizontal displacements and vertical displacement, respectively.

Wave equation (Holdsworth and Glynn, 1978):

$$\frac{\partial^2 W_b}{\partial t^2}=\frac{1}{\rho_w}\frac{\partial}{\partial x}\left(d_0(x,y)\frac{\partial P'}{\partial x}\right)+\frac{1}{\rho_w}\frac{\partial}{\partial y}\left(d_0(x,y)\frac{\partial P'}{\partial y}\right)$$

where d_0 is sub-ice channel height; P' is pressure perturbations in sub-ice water

Boundary conditions

Boundary conditions at ice-shelf base (as the example of the used approximation) ($z=h_b(x,y)$):

$$\begin{cases} \left(\dfrac{\partial \sigma_{xx}}{\partial x}\right)^{N_\xi}+\left(\eta'_x\dfrac{\partial \sigma_{xx}}{\partial \eta}\right)^{N_\xi}+\left(\xi'_x\dfrac{\partial \sigma_{xx}}{\partial \xi}\right)^{N_\xi}+\left(\eta'_y\dfrac{\partial \sigma_{xy}}{\partial \eta}\right)^{N_\xi}+\left(\xi'_y\dfrac{\partial \sigma_{xy}}{\partial \xi}\right)^{N_\xi}- \\ -\dfrac{1}{H}\dfrac{1}{\Delta\xi}\left\{\sigma_{xx}\dfrac{\partial h_b}{\partial x}+\sigma_{xy}\dfrac{\partial h_b}{\partial y}+P'\dfrac{\partial h_b}{\partial x}\right\}^{N_\xi}+\dfrac{1}{H}\dfrac{1}{\Delta\xi}\sigma_{xz}^{N_\xi-1}= \\ =\dfrac{1}{\Delta\xi}\dfrac{\partial h_b}{\partial x}\rho\, g+\rho\dfrac{\partial^2 U_b}{\partial t^2}; \\ \left(\dfrac{\partial \sigma_{yx}}{\partial x}\right)^{N_\xi}+\left(\eta'_x\dfrac{\partial \sigma_{yx}}{\partial \eta}\right)^{N_\xi}+\left(\xi'_x\dfrac{\partial \sigma_{yx}}{\partial \xi}\right)^{N_\xi}+\left(\eta'_y\dfrac{\partial \sigma_{yy}}{\partial \eta}\right)^{N_\xi}+\left(\xi'_y\dfrac{\partial \sigma_{yy}}{\partial \xi}\right)^{N_\xi}- \\ -\dfrac{1}{H}\dfrac{1}{\Delta\xi}\left\{\sigma_{yx}\dfrac{\partial h_b}{\partial x}+\sigma_{yy}\dfrac{\partial h_b}{\partial y}+P'\dfrac{\partial h_b}{\partial y}\right\}^{N_\xi}+\dfrac{1}{H}\dfrac{1}{\Delta\xi}\sigma_{yz}^{N_\xi-1}= \\ =\dfrac{1}{\Delta\xi}\dfrac{\partial h_b}{\partial y}\rho\, g+\rho\dfrac{\partial^2 V_b}{\partial t^2}; \\ \left(\dfrac{\partial \sigma_{zx}}{\partial x}\right)^{N_\xi}+\left(\eta'_x\dfrac{\partial \sigma_{zx}}{\partial \eta}\right)^{N_\xi}+\left(\xi'_x\dfrac{\partial \sigma_{zx}}{\partial \xi}\right)^{N_\xi}+\left(\eta'_y\dfrac{\partial \sigma_{zy}}{\partial \eta}\right)^{N_\xi}+\left(\xi'_y\dfrac{\partial \sigma_{zy}}{\partial \xi}\right)^{N_\xi}- \\ -\dfrac{1}{H}\dfrac{1}{\Delta\xi}\left\{\sigma_{zx}\dfrac{\partial h_b}{\partial x}+\sigma_{zy}\dfrac{\partial h_b}{\partial y}-P'\right\}^{N_\xi}+\dfrac{1}{H}\dfrac{1}{\Delta\xi}\sigma_{zz}^{N_\xi-1}= \\ =\rho\, g-\dfrac{1}{\Delta\xi}\rho\, g+\rho\dfrac{\partial^2 W_b}{\partial t^2}. \end{cases}$$

3. Numerical experiments

Ice shelf length is equal to 3 km

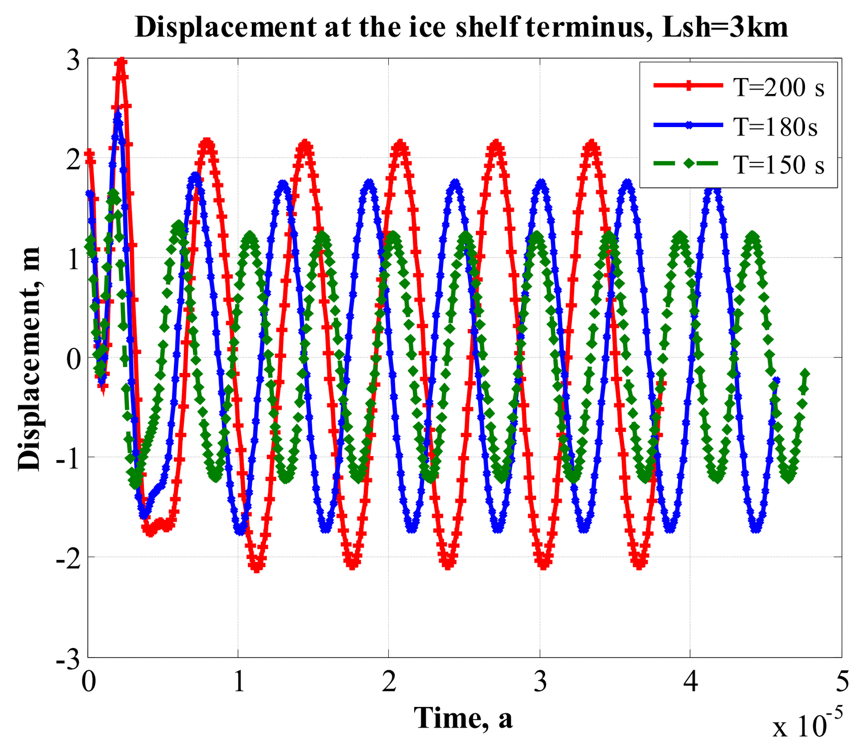

Fig. 2. The histories of ice-shelf terminus deflection obtained for the incident ocean waves in the "infragravity" part of the spectrum (the term "infragravity" was introduced in (Bromirski et al., 2010)). The amplitude of the incident wave is equal to 1 m.

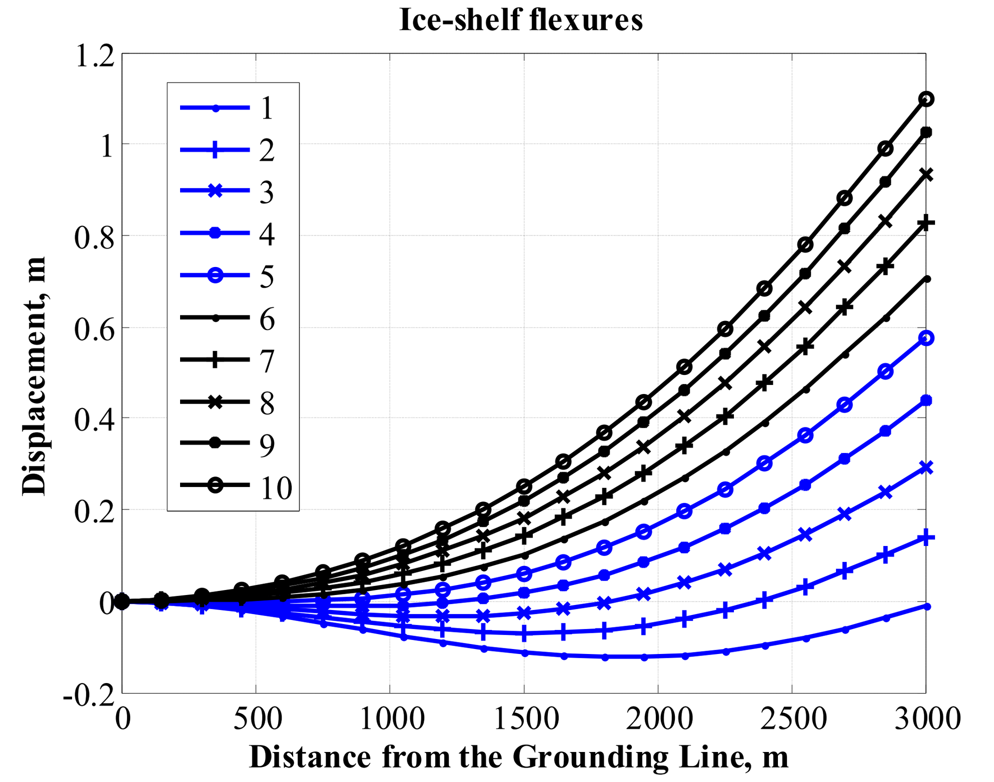

Fig. 3. Successive ice-shelf deflection profiles. L_{sh}=3km. The period of the forcing is equal to 150s, the amplitude of the incident wave is equal to 1 m.

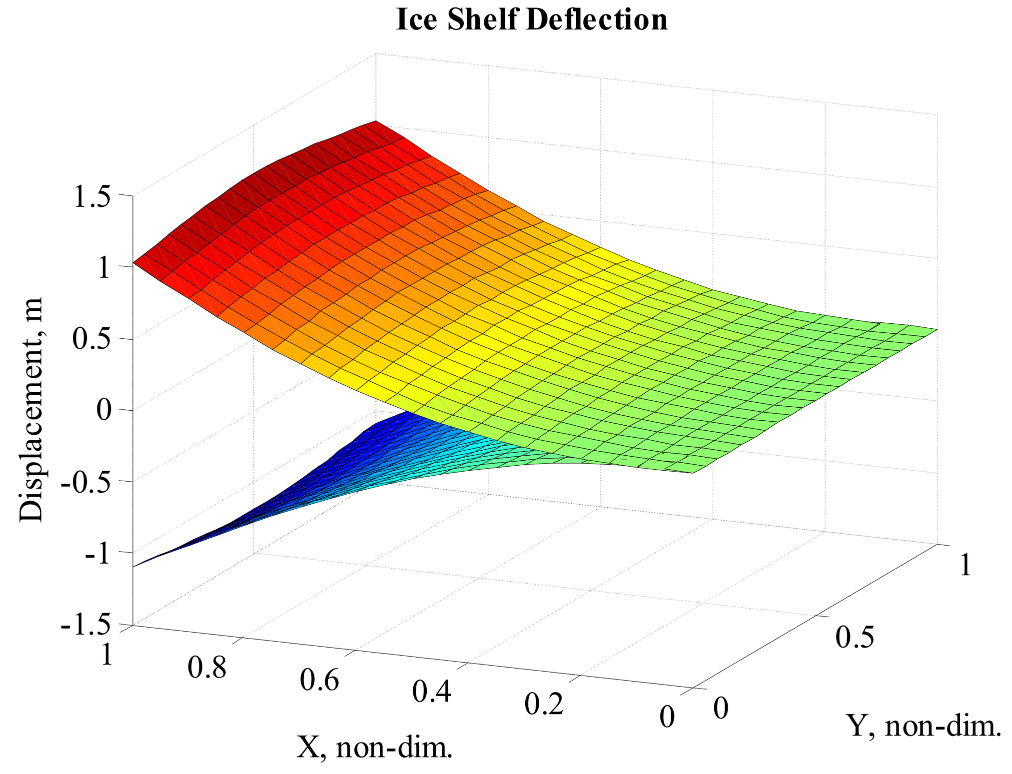

Fig. 4. Ice-shelf maximal and minimal deflections, respectively. L_{sh}=3km. The period of the forcing is equal to 150s, the amplitude of the forcing is equal to 1m.

Ice shelf length is equal to 5 km

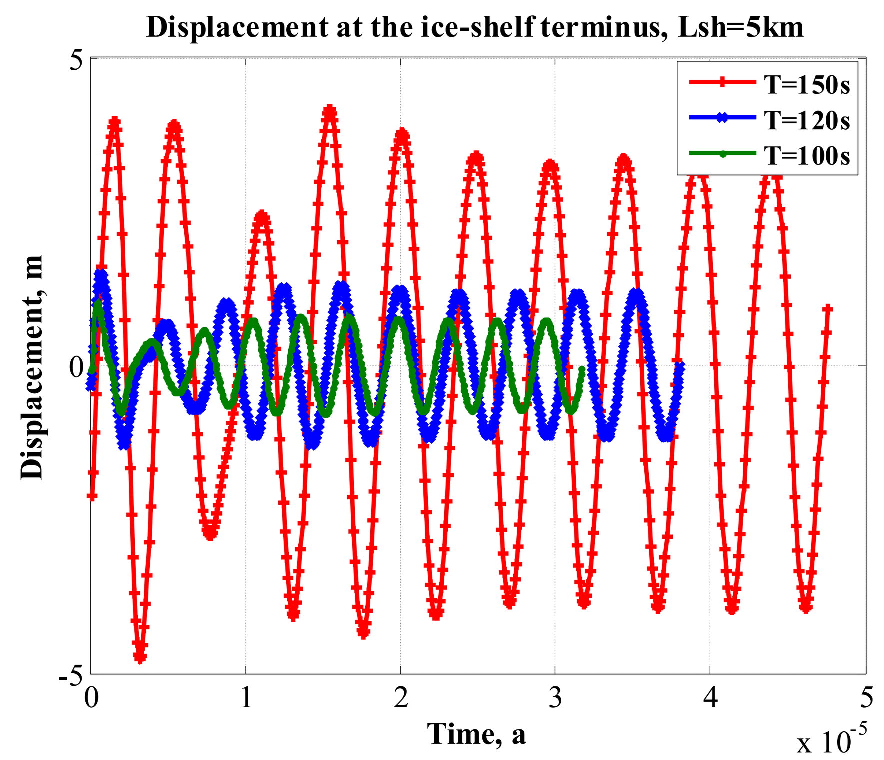

Fig. 5. The histories of ice-shelf terminus deflection obtained for the incident ocean waves in the "infragravity" part of the spectrum (Bromirski et al., 2010). The amplitude of the incident wave is equal to 1 m.

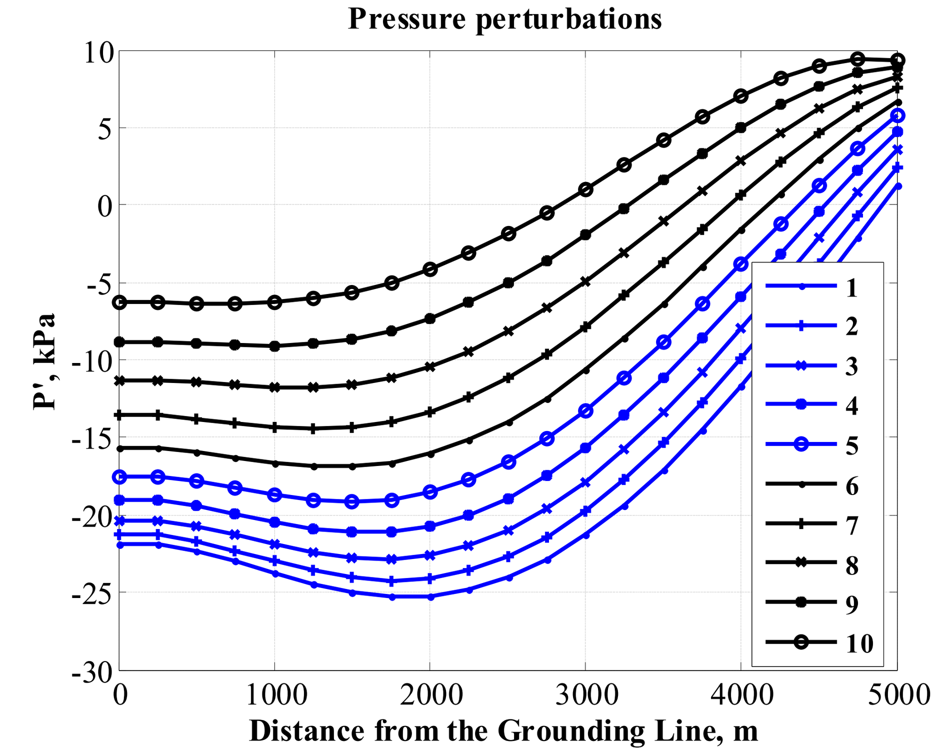

Fig. 6. Successive profiles of the pressure perturbations along the center-line. L_{sh}=5km. The period of the forcing is equal to 100s, the amplitude of the incident wave is equal to 1 m.

Ice shelf length is equal to 9 km

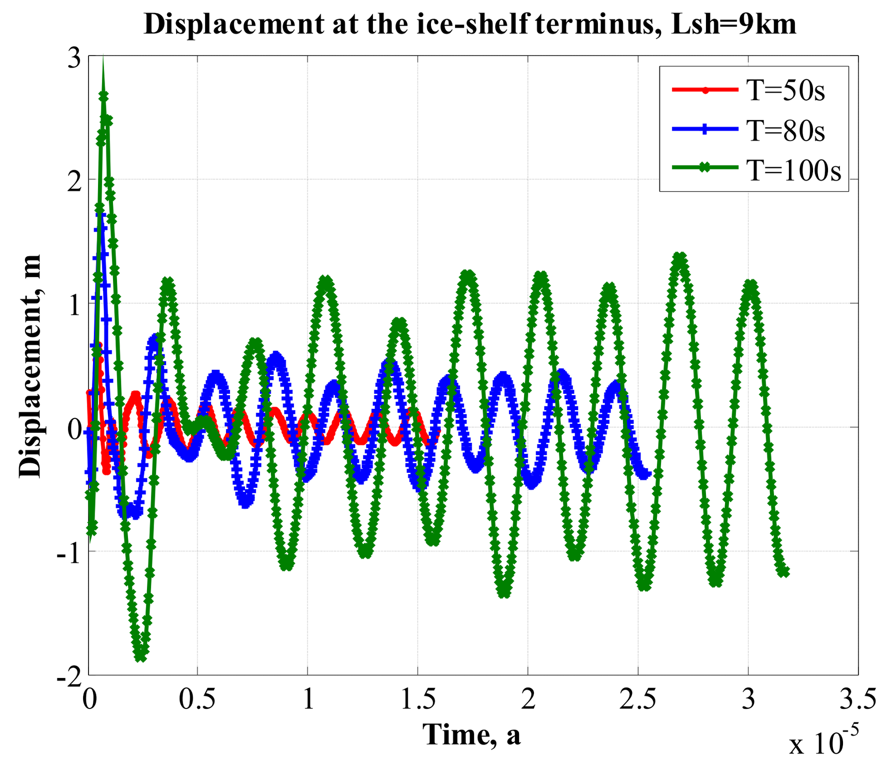

Fig. 7. The histories of ice-shelf terminus deflection obtained for the incident ocean waves in the "infragravity" part of the spectrum (Bromirski et al., 2010). The amplitude of the incident wave is equal to 1 m.

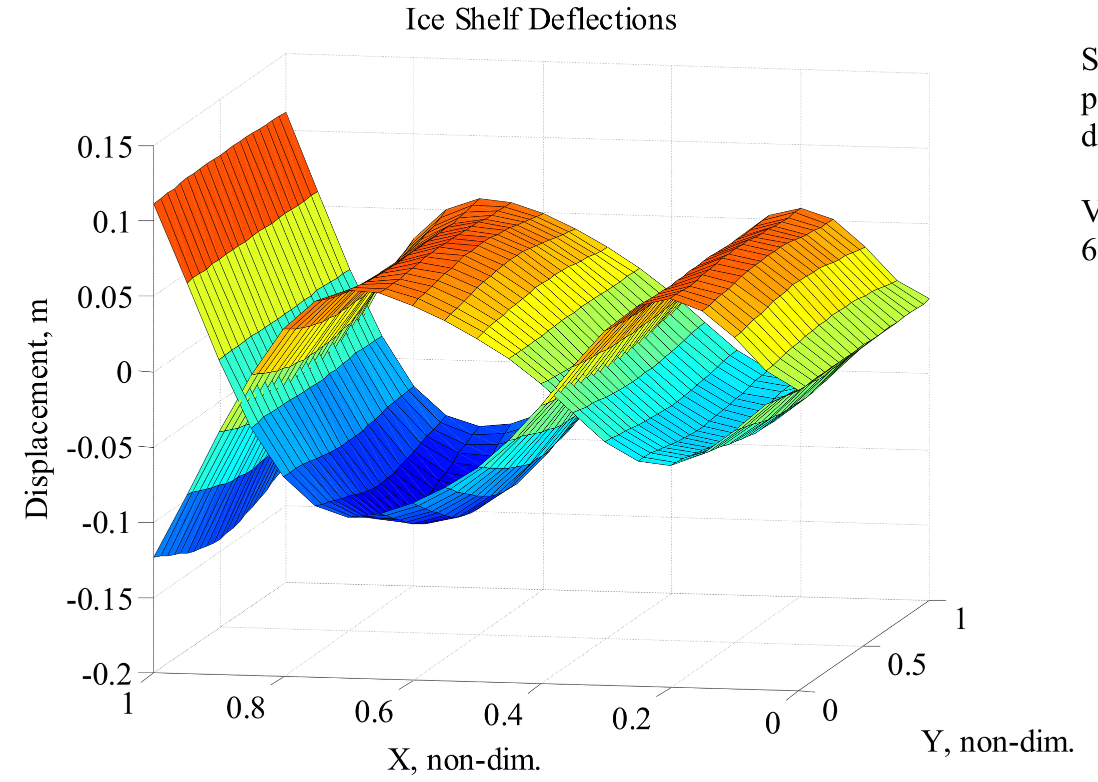

Fig. 8. Ice-shelf deflections. L_{sh}=9km. The period of the forcing is equal to 50s, amplitude of the forcing is equal to 1m.

4. Summary

The numerical simulation has shown that the modelling of the ice-shelf vibrations can be performed in the full model, which links well known momentum equations with the wave equation for non-viscous fluid, i.e. for sub-ice sea water. Nevertheless, the numerical simulation reveals that the numerical stability requires the application of an additional method of the numerical approximation. On the other hand, in contrariety to the Holdsworth & Glynn model (thin-plate model), ice-shelf vibrations not always follow for the incident wave in the full model. "Not always follow" means that incident ocean waves induce cyclical ice-shelf deflections with the same frequency, but the deflection amplitude (in non-resonance case) is not equal to the one in the incident wave. Evidently, the explanation can be given from the point of view of the elastic medium deformation theory. Exactly, the full model considers a common elastic medium deformation, which implies that there is a distinction in the deformations of different horizontal layers in the medium. Thus, the three stress components σ_{xz}, σ_{yz}, σ_{zz} are non-zero. This forcing complementary hampers the deflections of the plate. In other words, the plate described by the full model is anticipated to be more rigid in comparison with the thin plate, which is described by the thin plate model.

References

Bassis J.N., Fricker H.A., Coleman R., Minster J.-B.: An investigation into the forces that drive ice-shelf rift propagation on the Amery Ice Shelf, East Antarcyica. J. of Glaciol. 54 (184): 17-27, 2008.

Bromirski P.D., Sergienko O.V., and MacAyeal D.R.: Transoceanic infragravity waves impacting Antarctic ice shelves. Geophys. Res. Lett. 2009; 37: L02502, doi:10.1029/2009GL041488.

Holdsworth G and Glynn J.: Iceberg calving from floating glaciers by a vibrating mechanism. Nature. 274, 464-466, 1978.

Goodman D.J., Wadhams P. and Squire V.A.: The flexural response of a tabular ice island to ocean swell. 1980; Ann. Glaciol., 1: 23–27.

Konovalov Y. V.: Ice-shelf resonance deflections modelled with a 2D elastic centre-line model. Physical Review & Research International, 4(1), 9-29, 2014.

Landau LD, Lifshitz EM. Theory of Elasticity. Vol. 7. 3rd ed. Butterworth-Heinemann; 1986.

Lurie AI. Theory of Elasticity. Springer; 1999.

Reeh N., Christensen E.L., Mayer C., Olesen O.B.: Tidal bending of glaciers: a linear viscoelastic approach. Ann. Glaciol. 2003; 37: 83–89.

Schulson E.M.: The Structure and Mechanical Behavior of Ice. JOM. 1999; 51 (2): 21-27.

Sergienko O.V.: Elastic response of floating glacier ice to impact of long-period ocean waves. J. Geophys. Res. 2010; 115, F04028, doi:10.1029/2010JF001721.

Vaughan D.G.: Tidal flexure at ice shelf margins. J. Geophys. Res. 100(B4), 6213-6224, 2002.